Rheology of reconstituted type I collagen gel in confined compression

David M. Knapp, Victor H. Barocas, and Alice G. Moon[a)]

Department of Chemical Engineering and Materials Science, University of Minnesota, Minneapolis, Minnesota 55455

Kyeongah Yoo and Linda R. Petzold

Department of Computer Science, University of Minnesota, Minneapolis, Minnesota 55455

Robert T. Tranquillo[b)]

Department of Chemical Engineering and Materials Science, University of Minnesota, Minneapolis, Minnesota 55455

(Received 10 October 1996; final version received 10 June 1997)

Synopsis

Collagen gels are used extensively for studying cell–matrix mechanical interactions and for making tissue equivalents, where these interactions lead to bulk deformation of the sparse network of long, highly entangled collagen fibrils and syneresis of the interstitial aqueous solution. We have used the confined compression test in conjunction with a biphasic theory to characterize collagen gel mechanics. A finite element method model based on our biphasic theory was used to analyze the experimental results. The results are qualitatively consistent with a viscoelastic collagen network, an inviscid interstitial solution, and significant frictional drag. Using DASOPT, a differential-algebraic equation solver coupled with an optimizing algorithm, the aggregate modulus for the collagen gel was estimated as 6.32 Pa, its viscosity as 6.6×10^4 Pa s, and its interphase drag coefficient as 6.4×10^9 Pa s m^{-2} in long-time (5 h) creep. Analysis of short-time (2 min) constant strain rate tests gave a much higher modulus (318.3 Pa), indicating processes that generate high resistance at short time but relax too quickly to be significant on a longer time scale. This indication of a relaxation spectrum in compression is consistent with that characterized in shear based on creep and dynamic testing. While Maxwell fluid behavior of the collagen network is exhibited in shear as in compression, the modulus measured in shear was larger. This is hypothesized to be due to microstructural properties of the network. Furthermore, parameter estimates based on the constant strain rate data were used to predict accurately the stress response to sinusoidal strain up to 15% strain, defining the linear viscoelastic limit in compression. © *1997 The Society of Rheology.* [S0148-6055(97)01205-4]

[a)]Current affiliation: Eastman Kodak Company, Rochester, NY.

[b)]Address correspondence to R.T.T. at Dept. of Chemical Engineering and Materials Science, 151 Amundson Hall, University of Minnesota, Minneapolis, MN 55455-0132. Electronic mail: tranquillo@cems.umn.edu

© 1997 by The Society of Rheology, Inc.

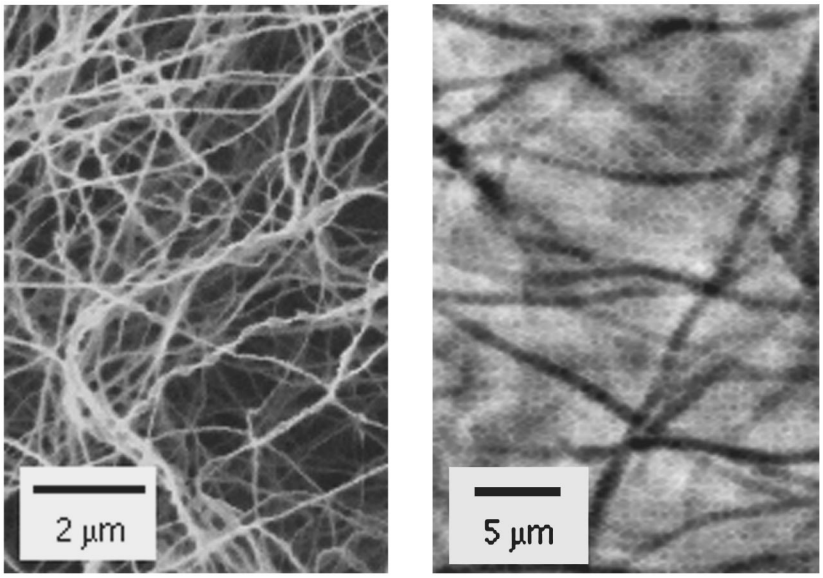

FIG. 1. Reconstituted type I collagen gel. SEM (a) and light microscopic (b) images show that collagen gel consists of two phases: an entangled fibrillar network surrounded by aqueous solution. The gel is in the hydrated state of the rheological tests in (b).

I. INTRODUCTION

The engineering of tissue analogs, such as bioartificial skin [Bell *et al.* (1981)] and artery [Weinberg and Bell (1986); Tranquillo *et al.* (1996)], based on entrapping cells in reconstituted type I collagen gel has become an active area of research in recent years, as has the use of such ''tissue equivalents'' in fundamental studies of cell behavior [Bell *et al.* (1979); Grinnell (1991); Moon and Tranquillo (1993)]. An inherent property of tissue equivalents is the consolidation of the collagen network resulting from traction exerted by the cells, a cell-induced syneresis of the gel. Therefore, characterizing the mechanical behavior of collagen gel is essential but has received relatively little attention until now.

Collagen gel behavior results from the intrinsic properties of and interaction between two component phases: a network of collagen fibrils and interstitial solution, typically, tissue culture medium. The fibrils form a sparse ($<$ 1% vol) but highly entangled network [Allen *et al.* (1984)] (Fig. 1) that effectively resists shear and extension but has little compressive strength. Resistance to the interstitial flow of the solution through the network, however, can lead to high solution pressures, which allow the gel to withstand compressive loads. Thus, when the gel is subjected to shear or tension, the physically crosslinked network supports virtually all of the load; under compression, however, the network transfers much of the load to the interstitial solution, the incompressibility of which prevents network collapse.

Fibrin gel and articular cartilage, both of which have entangled fibrillar networks similar to collagen gel, have been studied in some detail and provide a valuable basis for our study. Fibrin gel rheology in shear has been studied extensively by Ferry and coworkers [e.g., Bale *et al.* (1985)]. Collagen gel, like fibrin gel, shows shear rheology that can be characterized as a Maxwell fluid in long-time (hours) creep [Barocas *et al.* (1995)], with a zero-shear viscosity of 7.4×10^5 Pa s and a shear modulus of 15.5 Pa.

Shear rheology is not sufficient, however, to characterize fully the gel mechanics. In shear, the network and solution phases essentially deform together, so no information can be gained about the consequence of interstitial flow described earlier, that is, the magnitude of interphase drag. In the confined compression test, a sample confined within an impermeable cup is compressed by a rigid, hightly permeable porous piston. Since the solution can permeate out through the piston but the network cannot, there is relative motion of the two phases. We have adapted this test used by Mow and co-workers in studying articular cartilage [Holmes (1986); Kwan *et al.* (1990); Setton *et al.* (1993)] to study collagen gel, where the collagen network of the gel exhibits fluid behavior in long-time loading in contrast to the solid behavior for cartilage. Our biphasic theory [Barocas and Tranquillo (1997b)], based on that adapted by Dembo and Harlow (1986) from the volume averaging theory of Drew and Segel (1971), was used to obtain optimal estimates of the shear modulus, viscosity, and drag coefficient for the collagen network in confined compression for reconstituted type I collagen gel.

II. MATERIALS AND METHODS

A. Solution for reconstitution of type I collagen gel

All rheological testing was conducted on gels reconstituted using Vitrogen 100 type I collagen (Collagen Corporation, No. 0701-IN), a solution of 99.9% pure pepsin-digested bovine dermal collagen dissolved in 0.012 N HCl at a concentration of 3.0 mg/ml. It consists of 95%–98% type I collagen (mainly monomeric) with the remainder being type III collagen. The solution was prepared similarly to that previously used for assays of cell–matrix mechanical interactions [Barocas *et al.* (1995)] with the substitution of $1\times$ Gibco Medium 199 (M199) for fetal bovine serum. A combination of 20 μl 1M HEPES buffer solution, 132 μl 0.1 N NaOH, 100 μl $10\times$ MEM, 60 μl $1\times$ M199, 1 μl penicillin–streptomycin solution (5000 units of penicillin and 5000 μg streptomycin/ml in 0.85% saline solution), 10 μl L–glutamine solution made from 29.2 mg/ml in 0.85% saline solution, and 677 μl Vitrogen 100 collagen was used to prepare 1 ml of a collagen solution. All reagents were kept in an ice bath during preparation. The final concentration of collagen was 2.0 mg/ml at physiological pH (7.4). Light microscopic imaging of collagen gel was performed on a Zeiss Axiovert 10 using a $\times$ 40 objective in combination with a $\times$ 2.5 Optovar lens and long distance (LD) condenser [Guido and Tranquillo (1993)]. Scanning electron microscope (SEM) imaging of glutaraldehyde fixed collagen gel was performed at $\times$ 10 000 total magnification using previously described methods [Heath and Hedlund (1984)].

B. Confined compression: Apparatus and collagen gel preparation

Rheological measurements of the collagen gel in uniaxial confined compression were conducted on a Chatillon Vitrodyne V200 biomechanical testing system. The V200 allows computer-controlled force-length compression/extension data to be obtained for specimens maintained in cell culture conditions. The configuration of the V200 for confined compression is shown in Fig. 2. The gel was compressed between a piston of high porosity (several orders of magnitude higher than the gel) and a nonadhesive, impermeable cup. Network and solution flows were confined by the sides of the cup so that the deformation was solely in the axial direction. Force readings were measured by load cells located on the shims based on their deflection, and length was measured using a linear variable-differential transformer position transducer. Changes in the length/loading of the mounted gel were effected by the opening and closing of a stepper-motor-controlled air bellows.

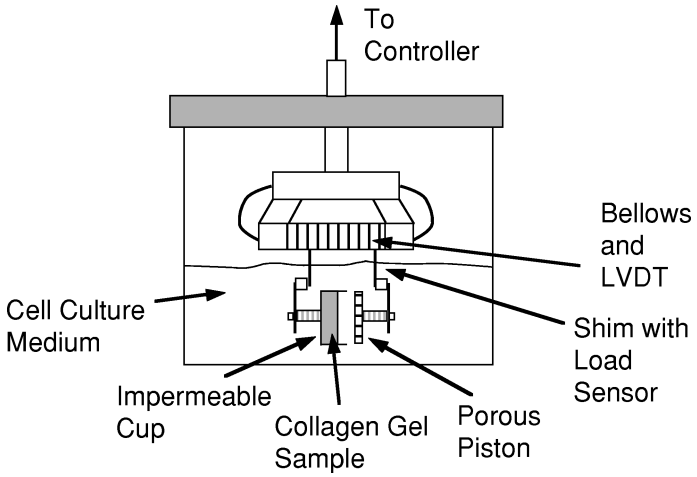

FIG. 2. Chatillon Vitrodyne V200 in confined compression. The external pneumatic control system combined with load sensors on the hanging shims allow stress/strain measurements to be conducted in a cell culture environment.

The confined compression chamber consisted of a cylindrical impermeable acrylic cup (38 mm diam) mounted directly opposite a piston (37 mm diam) made of porous polyethylene (80 μm average pore size, Bel-Art Products) mounted on an acrylic support. The bottom of the cup was coated with a thin layer of porous polyethylene to anchor the collagen gel to the base of the cup by allowing penetration of network fibrils formed during gel preparation. Collagen gels were prepared in the chamber by one of the two following methods.

For the ramp and dynamic tests, the forcing frame of the V200, with the confined compression end pieces attached, was placed in an incubator maintained at 37 °C such that the cup was positioned open end up. Then, 5.0 ml of prepared collagen solution was pipetted into the cup. The bellows were deflated so that the piston rested on the surface of the collagen solution. A thin layer of silicone oil was placed around the 500 μm gap between the cup and the edge of the piston to minimize evaporation from the solution. The sample was incubated for 1 hr at constant length over which time fibrillogenesis occurred and the solution gelled. Then, the gel sample was completely submerged in 425 ml of M199 at 37 °C and was allowed to equilibrate held at a constant length for 3 hr in a 37 °C incubator.

For the creep tests, the significantly longer test times necessitated a sterile procedure. First, 5.0 ml of prepared collagen solution was aseptically pipetted into the cup and covered with a Teflon cap. This ''mold'' was then incubated at 37 °C for 1.5 h. After removing the Teflon cap, the cup, containing the collagen gel, was mounted onto the V200 in aseptic conditions, subsequently submerged in 425 ml of sterile phosphate buffered saline (PBS) (Gibco) at 37 °C and was allowed to equilibrate held at a constant length for 9 hr in a 37 °C incubator. The longer equilibration time was required to ensure the smaller applied force was accurate. Ramp tests performed on gels incubated in PBS instead of M199 yielded similar estimates of the rheological parameters described below (data not shown). Finally, the system compliance was accounted for since the V200 measurements include a calibrated shim bend correction. Mount compliance was negligible compared to collagen gel, as determined by placing the piston in contact with the cup base (data not shown).

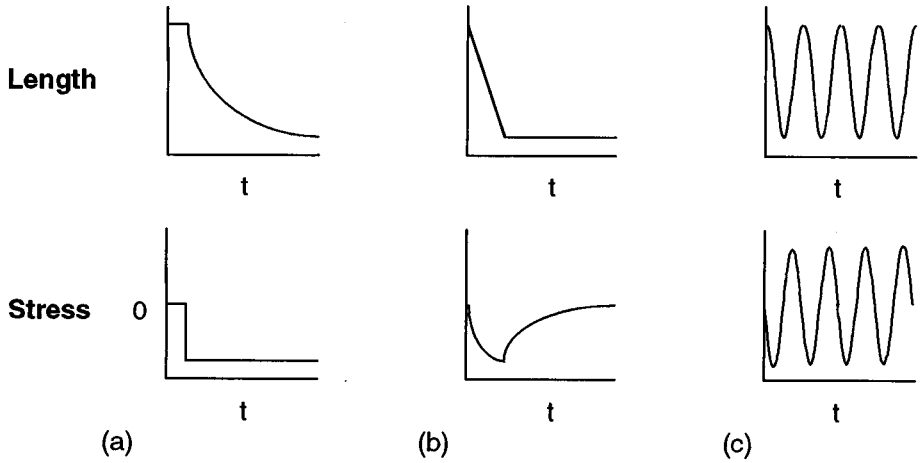

FIG. 3. Schematic of small-strain tests in confined compression. The gel length decreases in response to a constant imposed load in creep (a), while the stress responses to constant strain rate (b) and sinusoidal (c) deformations are shown.

To determine the extent to which the network was forced through piston pores or the gap between the piston and the cup, several tests were repeated using modified pistons in which both the pore size and gap width were halved. The results from these tests were identical to those performed with the standard piston, indicating that the network flow through or around the piston was negligible. In addition, no bulging through the gap was observed in any test except when an impermeable piston was used.

C. Confined compression: Mechanical tests

Three compression tests were conducted on the collagen gel using the V200: creep, constant strain rate (ramp), and sinusoidal strain (dynamic). A qualitative representation of the experiments is shown in Fig. 3. In creep, a constant compressive force was applied on the gel, and the length of the gel was measured over time. For the ramp test, the length was shortened at a constant rate to a prescribed value and then held at a constant length, whereas in the dynamic test, the gel was deformed sinusoidally between its initial length and a prescribed minimum length, the resultant force being measured in both cases. Data were obtained by a dedicated computer at intervals of 1 s.

Creep tests were performed using the controlled force mode of the V200. A constant compressive stress $\sigma = 0.43$ or 0.80 Pa was applied to the gel based on the applied forces of 4.9×10^{-4} and 9.0×10^{-4} N, respectively and a sample area of 11.3 cm^2. Creep tests were stopped before the strain exceeded 15% given the previously determined linear viscoelastic limit (LVE) of 10% in shear [Barocas *et al.* (1995)] (strain ϵ was calculated as $1 - L/L_0$ and creep compliance as ϵ/σ_0). All of the creep results were obtained on previously untested gels.

Ramp tests were performed using the controlled length mode of the V200. Gels were compressed at a constant rate for 120 s to 10% strain. For the remainder of the test, the gels were held at a constant length as force measurements continued. All of the ramp results were also obtained on previously untested gels. In addition, four tests were performed on the same collagen gel to assess repeatability.

Dynamic tests were performed in the controlled length mode by increasing the amplitude of the sinusoidal strain to a desired value (e.g., 2%) at a frequency of 4.2×10^{-3} Hz (period of 240 s). Sinusoidal strain at that amplitude was maintained until the force response in the gel had reached a steady periodic profile. The amplitude was then increased to the next higher value (e.g., 4%) with the steady dynamic data again being acquired. This procedure was repeated up to 30% strain, and then the amplitude was reduced back to 2% strain for a final reading. At strains higher than 30%, the positive stresses observed near the 0% strain region of the cycle dropped to zero during the course of the test, indicating a breakdown of the integrity of the collagen/piston anchorage.

D. Shear: Apparatus, collagen gel preparation, and tests

Oscillatory shear testing was conducted with a Rheometrics, Inc. (Piscataway, NJ) Fluids Spectrometer (RFSII) in the concentric cylinder (Couette) geometry. The sample was prepared by mixing 14 ml of collagen solution and pouring it into the bottom fixture. The cup was preheated to 37 °C and maintained at 37 °C ($\pm$0.5 °C) by a recirculating fluids bath with proportional controller to induce fibrillogenesis. The bob (16 mm in diameter and 33 mm in length) was immediately lowered into the solution (the gap between the cup and the bob was 1 mm), and the sample was left undisturbed for 3.5 h before testing to allow for development of the gel network. Fifteen minutes after the collagen solution was poured, mineral or silicone oil was added to the top of the sample to prevent drying. After the 3.5 h period, the sample was subjected to oscillatory shear by the rotating cup to a specified maximum strain amplitude. The dynamic moduli were then measured as a function of angular frequency using the 10 g cm torque transducer.

Creep in shear was measured with a Rheometrics, Inc. Stress Rheometer also in the Couette geometry. In these tests, 20 ml of collagen solution was mixed and poured into the preheated cup (37 °C), and the bob (13 mm in diameter and 40 mm in length) was immediately lowered into the solution (the gap between the cup and the bob was 1 mm). After 15 min, mineral or silicone oil was added to cover the top of the sample. After 3.5 h, a constant stress was applied (by the rotating bob, in this case) to the sample and the strain was monitored with time. The temperature was maintained at 37 °C ($\pm$0.5 °C) during the test.

III. DATA ANALYSIS

A. Confined compression

Because the confined compression test does not provide a homogeneous deformation, a constitutive model was required to analyze the data, and we applied our biphasic continuum theory for mechanics of tissue equivalents [Barocas and Tranquillo (1997b)]. The cell conservation equation and traction stress terms were omitted because the collagen gel used here was acellular, and the remaining equation set was reduced by the simplifying linear test geometry; only the axial (z) components of velocity and stress were nonzero. The resulting equation set was further reduced by eliminating the solution velocity and pressure using the total continuity equation and the solution phase momentum balance, respectively. The latter was simply Darcy's law given the assumption that the solution was inviscid (i.e., interphase frictional drag dominated intraphase viscosity). The effects of gravity were neglected. The confined compression test was, thus, modeled by two conservation equations and a constitutive equation. Conservation of the network is given by

$$\dot{\theta}+\frac{\partial v}{\partial z}\,\theta = 0, \tag{1}$$

where θ is the network volume fraction (equivalent to concentration because the two phases have approximately the same intrinsic density), and v is the network velocity. The dot represents the material derivative moving with the network based on v. Conservation of linear momentum, which reduces to a mechanical force balance in the creeping flow limit, is given by

$$\frac{\partial}{\partial z}[\sigma\theta]-\varphi_0\frac{\theta}{1-\theta}v = 0, \tag{2}$$

where σ is network viscoelastic stress and φ_0 is the interphase drag coefficient (inversely proportional to the Darcy's Law permeability of the gel). The weighting of σ by θ and the θ dependence of the drag term follow from the volume averaging theory of Drew and Segel (1971). Finally, the constitutive equation for the network stress was assumed to be that for a compressible Maxwell fluid based on its fit to creep data in shear [Barocas *et al.* (1995)],

$$\frac{1}{G_{cc}}\dot{\sigma}+\frac{1}{\eta}\sigma = \frac{\partial v}{\partial z}, \tag{3}$$

where G_{cc} and η are the aggregate modulus and viscosity for confined compression,

$$G_{cc} \equiv 2G\left(\frac{1-\nu}{1-2\nu}\right), \tag{4}$$

$$\eta \equiv 2\mu_0\left(\frac{1-\nu}{1-2\nu}\right), \tag{5}$$

and G and μ_0 are the shear modulus and viscosity, and ν is Poisson's ratio. These parameters are considered intrinsic to the network phase. Note that even if values of G and μ_0 estimated from shear data [Barocas *et al.* (1995)] are assumed to apply for confined compression, ν cannot be estimated; its estimation requires unconfined compression tests.

The boundary conditions depended on the specific test. In all cases, the boundary condition at $z = 0$ (the base of the cup) was no displacement of the network ($v = 0$). At $z = L(t)$ (the porous piston), either the stress (in the case of a creep test) or velocity (in the case of a ramp or sinusoidal test) was specified. Zero stress, uniform initial conditions were assumed for all tests.

Since the equations possess nonlinear couplings and do not admit an analytical solution, we used numerical solutions to fit experimental data. The spatial derivatives in Eqs. (1)–(3) were discretized using the standard Galerkin finite element method (FEM) and piecewise quadratic basis functions (Appendix), converting the partial differential equation (PDE) system into an ordinary differential equation (ODE) system. This ODE system was then solved numerically using the DASOPT program [Petzold *et al.* (1995)]. The DASOPT routine solves differential-algebraic equations and ODEs [Petzold (1983)], generates sensitivities of the solution to system parameters [Maly and Petzold (1996)], and uses a sparse nonlinear optimizer algorithm to determine optimal parameter estimates based on a user-specified objective function (sum of squared error in our problem) and any system constraints.

DASOPT was used to determine G_{cc}, η, and φ_0 for each creep and ramp test. The results of the dynamic tests were compared with *a priori* model predictions based on estimates of the same three parameters determined from the ramp tests as these were conducted on comparable time scales. Thus, the creep and ramp data were used to estimate model parameter values, and the dynamic data served to validate the parameter values and the model equations.

Five issues related to parameter estimation were addressed: the accuracy of the measured stresses and strains, the accuracy of the parameter estimates, the repeatability of the data (one sample retested), reproducibility of the data (multiple samples tested), and the sensitivity of the model fits to the parameter values. The experimental accuracy of the V200 strain measurements was within $\pm$ 1% for all tests, while the stress measurements were within $\pm$ 1% for the ramp and dynamic tests, but only within $\pm$ 10% for the creep tests. The repeatability was assessed by calculating the standard deviation of parameter estimates from multiple tests of a single sample. The accuracy and reproducibility of the parameter estimates were analyzed using contours of constant sum of squared error in $G_{cc} - \eta$ space (φ_0 held constant at the optimal value), error being defined as the difference between the predicted and measured stress or strain at the time of the measurement. The error level for the confidence contours was chosen by the following condition resulting in an exact ellipsoidal 95% boundary for the linear problem:

$$S(\alpha) = S(\hat{\alpha})\left\{1+\frac{p}{n-p}F(p,n-p,0.95)\right\}, \tag{6}$$

where S is the sum of squared error, α is the vector of parameters with the hat denoting the best fit values, p is the number of parameters, n is the sample number, and F denotes the value of the F distribution for a particular number of parameters and samples for the 95% confidence level. Linear goodness-of-fit theory assigns a confidence level to a given contour based on the error associated with the contour, the minimum error based on the optimal fit, and the number of data points used; thus, for example, one can be 95% confident that the actual parameter values lie within the 95% confidence contour [Draper and Smith (1981)]. Although the regression problem is nonlinear, contours that approximate the exact statistical confidence levels based on linear theory were computed.

B. Shear

In the region where the plot of log $J(t)$ versus log t can be represented by a straight line of slope m, $G(t)$ can be calculated from the approximate interrelation [Tschoegl (1989)],

$$G(t) = \frac{1}{J(t)}\frac{\sin \pi m}{\pi m}, \tag{7}$$

where $J(t)$ is the creep compliance and $G(t)$ is the relaxation modulus. The elastic or storage modulus, $G'(\omega)$, can then be found from [Ferry (1980)],

$$G'(\omega)|_{\omega = 1/t} = G(t)+H(\lambda)\psi(m_1)|_{\lambda = t}, \tag{8}$$

where $H(\lambda)$ is the spectral relaxation function, m_1 is the (negative) slope of a plot of log H versus log λ, and $\psi(m_1) = (\pi/2)\csc(m_1\pi/2) - \Gamma(m_1)$, where Γ is the gamma function. If m is small, $G(t) \cong 1/J(t)$ follows from Eq. (7), and it can, thus, be shown from Eq. (8) that (see also below)

$$G'(\omega) \cong \frac{1}{J(t)}, \tag{9}$$

where ω corresponds to $1/t$ [Gerth *et al.* (1974)].

The spectral relaxation function, $H(\lambda)$, can then, correspondingly, be determined using the first-order approximation formulas given by Ferry (1980),

$$H(\lambda) = A(m_1)G' \left.\frac{d \log G'}{d \log \omega}\right|_{\omega = 1/\lambda}, \tag{10}$$

where $A(m_1) = \sin(m_1\pi/2)/(m_1\pi/2)$, and

$$H(\lambda) = -M(m_1)G(t) \left.\frac{d \log G(t)}{d \log t}\right|_{t = \lambda}, \tag{11}$$

where $M(m_1) = 1/\Gamma(1 - m_1)$.

Equation (10) applies only if $m_1 < 1$, and Eq. (11) applies only for negative values of m_1. The calculations for converting G' and $G(t)$ to $H(\lambda)$ involved two steps. First, $H(\lambda)$ was approximated by setting M and A to unity, $H^0(\lambda)$. The slope of $H^0(\lambda)$ was then determined, and the appropriate corrections were made in $H(\lambda)$ by multiplying the $H^0(\lambda)$ by the ''correction factors,'' M and A. The instantaneous derivatives in Eqs. (10) and (11) were approximated by the slopes of the doubly logarithmic plots of $G'(\omega)$ versus ω and $G(t)$ versus t. The approximation Eq. (9) can, thus, be justified *a posteriori* by assuming the approximations of Eqs. (10) and (11) are valid and then determining that the term $H(\lambda)\psi(m_1)|_{\lambda = t}$ is negligible compared to $G(t)$.

IV. RESULTS

A. Confined compression: Creep tests

The creep behavior of collagen gel at short times in confined compression is qualitatively different from that measured in shear, as shown in Fig. 4. The steep increase in the compliance seen in shear creep is typical for a viscoelastic fluid and is due to the elastic contribution. However, the increase in the compliance for confined compression is much more gradual in comparison. This is attributed to the effect of significant interphase drag in the gel at short time.

A typical long-time creep compliance curve for collagen gel in compression at 0.43 Pa applied stress is shown as the data points in Fig. 5(a). The long-time behavior is similar to that seen for collagen gel in shear [Barocas *et al.* (1995)], with a constant rate of increase in the compliance, substantiating the assumption of the Maxwell fluid behavior expressed in Eq. (3). The solid line in Fig. 5(a) is the optimal fit of the model equations to the data. The scaled sensitivity of the piston velocity to the model parameters for this test is shown in Fig. 5(b). Both the modulus and drag coefficient are important in the first hour of the test. However, once steady creep is reached, the viscosity becomes the dominant parameter.

The accuracy of the experimental results was best at the highest stress level, since the creep experiments were all run near the lower limit of the force transducer of the V200. From this fit of the creep data for four collagen gels (three gels at 0.43 Pa and one gel at 0.80 Pa), we obtained the modulus, viscosity, and drag coefficient of the gel in compres-

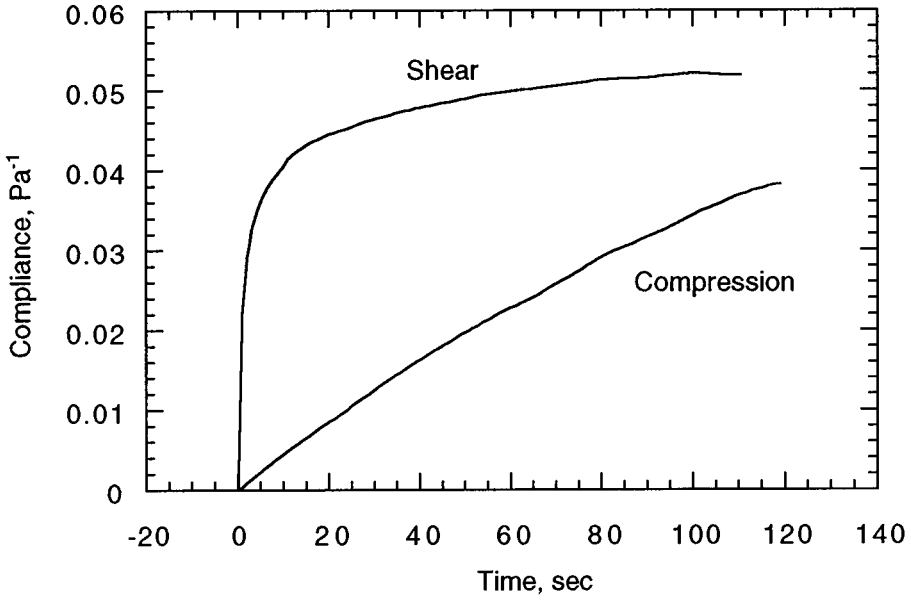

FIG. 4. Collagen gel creep compliance for compression vs shear. The gradual rise in the compliance in compression compared to shear (applied stress of 0.43 Pa, in both cases) is due to the resistance to the solution flow relative to the network fibrils in the confined compression test. The solution largely deforms with the network in shear.

sion for the time scale of 5 hr, shown in Table I. Variability in gel preparation leads to approximately 20%–50% uncertainty in these values as expressed by the standard deviation.

The 95% linear confidence regions for the 0.43 and 0.80 Pa creep tests are shown in Fig. 6. Although the contours do not exactly correspond to the linear confidence level, we can assess the relative magnitude of the errors due to the inaccuracy of the fit compared to the reproducibility of the results. The 95% contours are within 10% of the optimal values for G_{cc} and η. Therefore, the relative error of the fit is on the same order as the measurement errors for the stress. Since G_{cc} and η were both scaled by the applied stress when fitting the creep experiments, error in measured stress implies a linear increase in the size of the contours in both the η and G_{cc} directions.

The distance between the different contours is a measure of the level of reproducibility between creep tests of different samples. For the creep tests, the reproducibility of the experiment was poor since they were conducted near the lower limit of the force transducer resolution on the V200. The 95% confidence contours do not overlap; thus, no region of ''high probability'' could be extracted from the fits for determining an optimal set of values for G_{cc} and η. Therefore, we reported a mean value for the parameters.

B. Confined compression: Ramp tests

The relative motion between the network and interstitial solution can dominate the mechanics of the gel at shorter times at fixed sample sizes. Probing these interactions requires an experimental time frame on the order of a few minutes as compared to the long time scale in the creep tests. Therefore, we performed ramp compression tests, in which the gel was compressed to 10% strain at a constant rate for 120 s and then held at constant length. The stress trace from the run is shown as the data points in Fig. 7. The

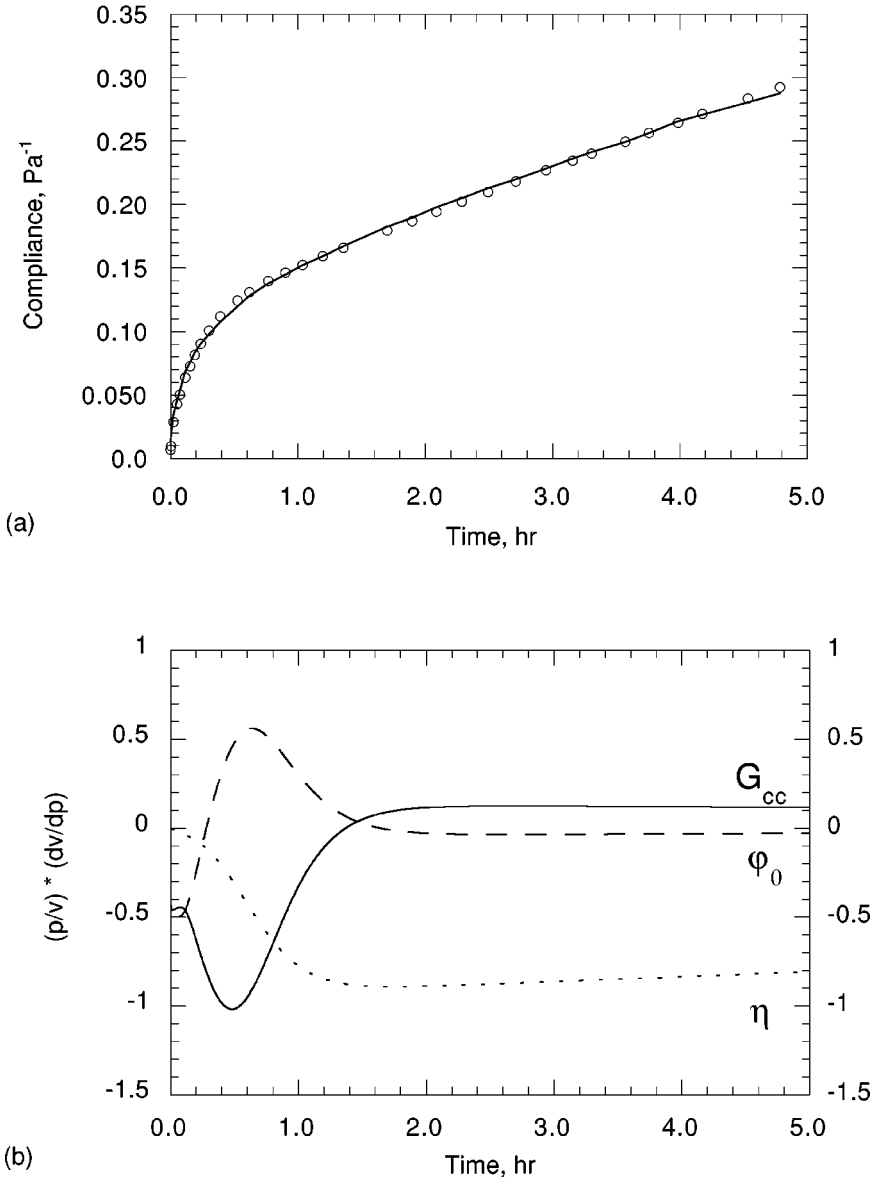

FIG. 5. Confined compression creep test results. (a) The long-time creep seen in confined compression is consistent with the Maxwell fluid behavior reported in shear. The data points (circles) were fit using the optimizing algorithm in DASOPT (solid line). (b) Sensitivity of the piston velocity to the model parameters for the test shown in (a) for the parameters $p = G_{cc}$, η, and φ_0.

compressive stress in the gel increases as the solution is forced out of the gel and the network is compressed. The stress drops once the gel has reached its final length as the network phase relaxes and the solution pressure in the gel equilibrates.

The data from the ramp test were fit using DASOPT, and the optimal parameter estimates are shown in Table II. As seen in Fig. 7, good agreement exists between the model fit and the data. The shorter time scale of the ramp tests leads to a much higher modulus as compared to the long-time creep tests. The value of the drag coefficient, however, was

TABLE I. Collagen gel confined compression creep parameters.

	Value	Standard deviation ($n = 4$)
Drag coefficient, $\varphi_0\theta_0$ (Pa s m^{-2})	6.4×10^9	$\pm$ 2.0×10^9
Aggregate viscosity, $\eta\theta_0$ (Pa s)	6.6×10^4	$\pm$ 3.2×10^4
Aggregate modulus, $G_{cc}\ \theta_0$ (Pa)	6.32	$\pm$ 0.91

similar to that estimated from long-time creep, as would be expected since φ_0 is likely independent of time scale, and the θ dependence of the drag term is accounted for in Eq. (2). Variability in the measurements between different collagen gels and for multiple ramp tests performed on the same gel was assessed. Parameter estimates for four repeated tests on the same sample varied less compared to estimates obtained from four different samples, as shown by a decreased standard deviation shown in Table II.

C. Confined compression: Dynamic tests, determination of the LVE limit, and model validation

In order to assess the LVE limit for the collagen network in compression, we performed strain sweeps by sinusoidally varying the length of the gel at 4.2×10^{-3} Hz ($T = 240$ s). The stress/strain response of the gel for varying strain levels is shown in Fig. 8(a). As the gel is compressed, the interstitial solution is exuded from the gel and the network deforms, creating negative stress. However, the stress increases and becomes positive as the gel is brought back to its initial length due to slight extension of the network after viscous flow during the instroke and solution flow into the gel. The width of the ellipses is an indication of the effects of viscous dissipation and solution flow from

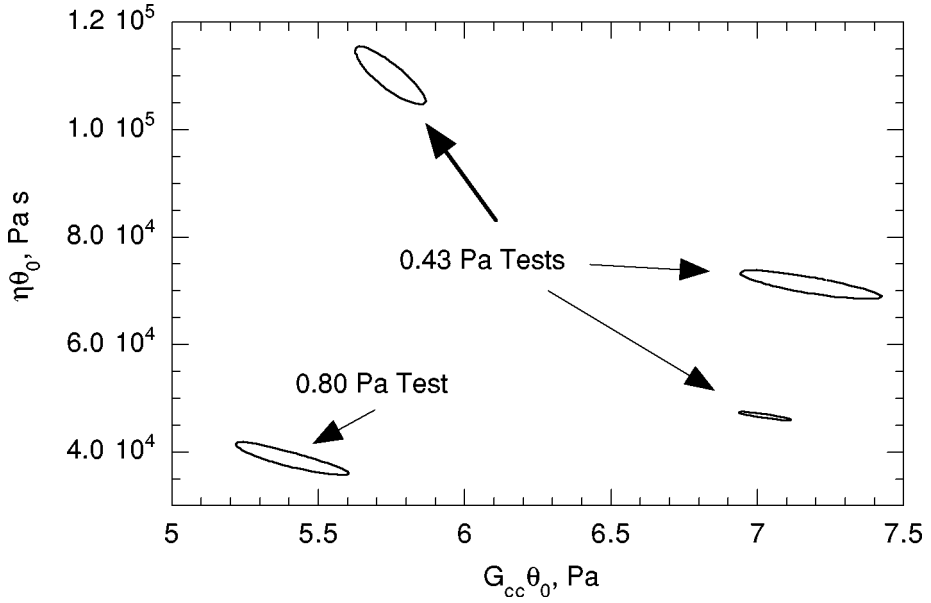

FIG. 6. Confidence contours for confined compression creep tests. The confidence regions for creep tests conducted at 0.43 and 0.80 Pa show the error due to the irreproducibility of the estimates between samples tested is much larger than that resulting from measurement or fitting inaccuracies.

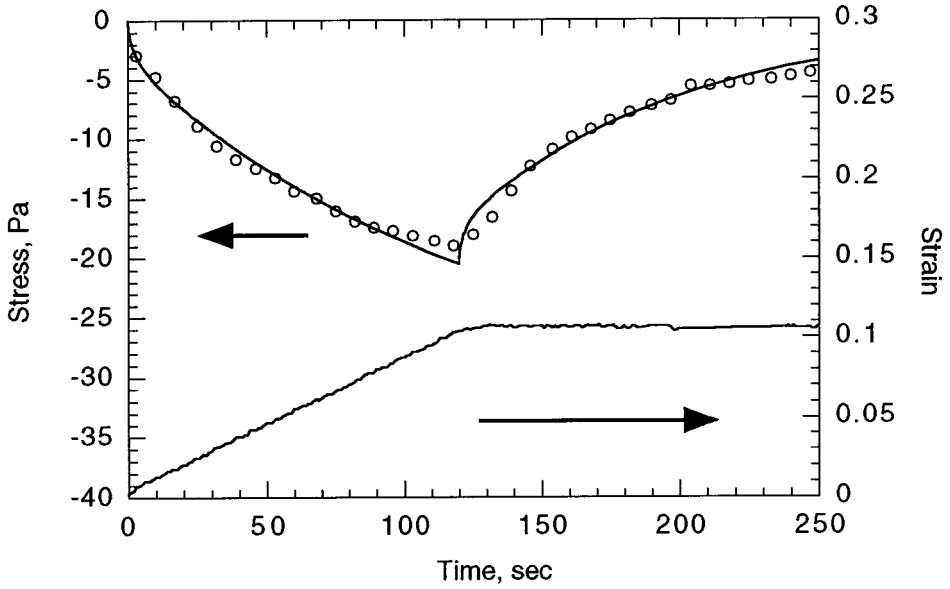

FIG. 7. Confined compression ramp test results. Parameter estimates for collagen gel in confined compression were obtained from fits of constant strain rate short-time ramp data. The gel was compressed to 10% strain at a constant strain rate over 120 s and then maintained at 10% strain (actual strain trace shown).

the gel. As the strain levels increase, the maximum and minimum stresses increase. The area within the ellipse represents the amount of energy dissipated in the gel during a cycle.

Figure 8(b) shows a comparison between the experimental stress response and that predicted by the biphasic model for the dynamic test using parameter estimates obtained from the 120 s ramp tests, which roughly approximate the time scale for the dynamic experiment with a 240 s period. Agreement is very good between the model prediction and the experiment, serving to validate the model for different modes of compressive deformations, which occur over similar time scales.

In order to determine the LVE limit, the expected maximum and minimum stresses are plotted over a strain range from 2% to 30% in Fig. 8(c) (data from two tests using different samples). The *a priori* model predictions based on the 120 s ramp test parameter estimates are also shown. Agreement between the data and the model predictions is very good up to 15% strain, at which point the model overpredicts considerably the measured stresses. This implies a LVE limit in compression of $\sim$ 15% as compared to $\sim$ 10% determined for shear.

TABLE II. Collagen gel confined compression ramp parameters.

	Value	Std Dev ($n = 4$)	Std Dev ($n = 1, 4$ tests)
$\varphi_0\theta_0$ (Pa s m^{-2})	1.2×10^9	$\pm$ 0.4×10^9	$\pm$ 0.2×10^9
$\eta\theta_0$ (Pa s)	3.1×10^4	$\pm$ 1.0×10^4	$\pm$ 0.4×10^4
G_{cc} θ_0 (Pa)	318.3	$\pm$ 34.0	$\pm$ 10.2

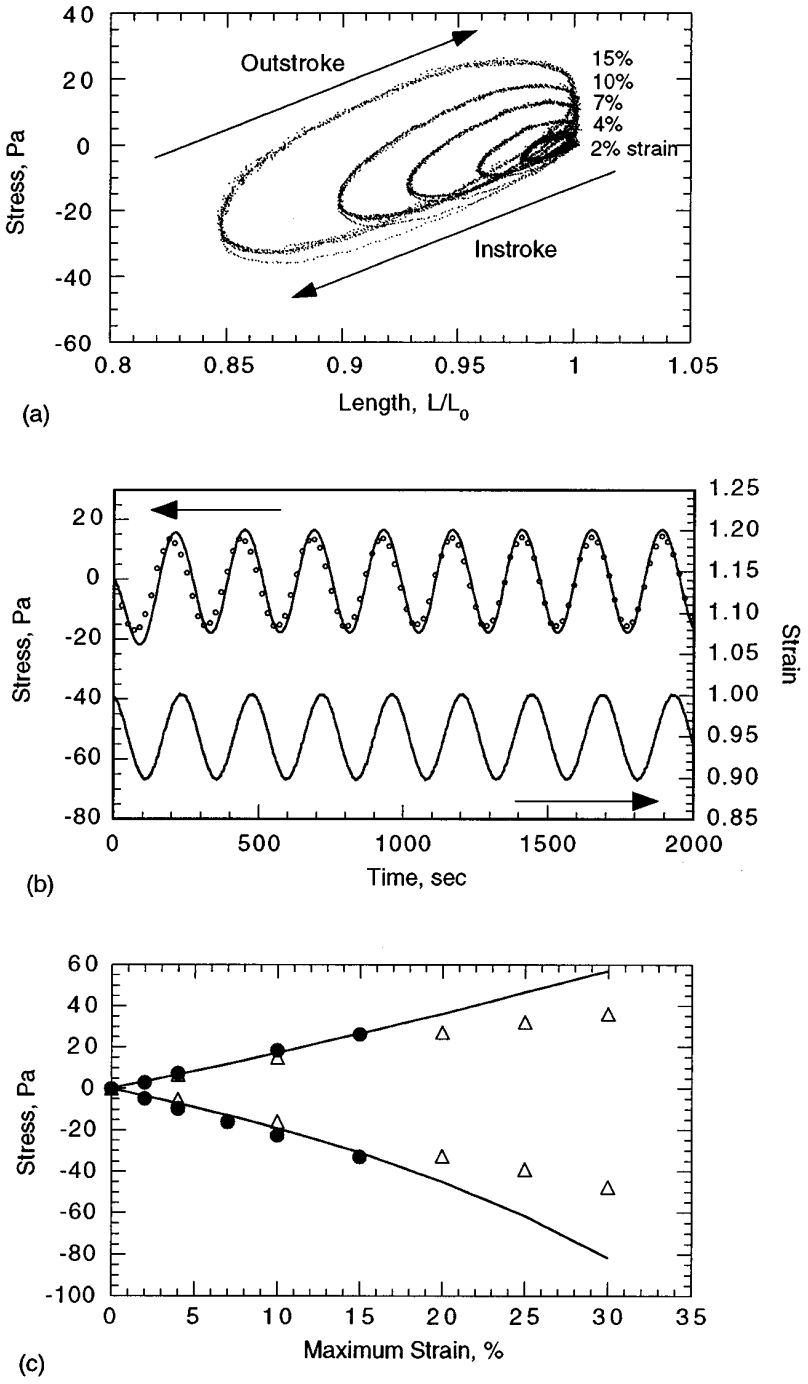

FIG. 8. Confined compression dynamic test results. (a) A collagen gel was subjected to a strain sweep from 2% to 15% strain using a period of 240 s. The elliptical shape of the stress strain curve is attributed to the effects of interstitial flow and viscous dissipation at short times. (b) Model predictions for the average stress based on parameter estimates determined in the ramp tests agree well with the data (actual strain trace shown). (c) The maximum and minimum stresses from two strain sweeps (denoted by filled circles and open triangles) are plotted against model predictions, which match the data well up to strains of 15%, validating our LVE assumption up to this strain.

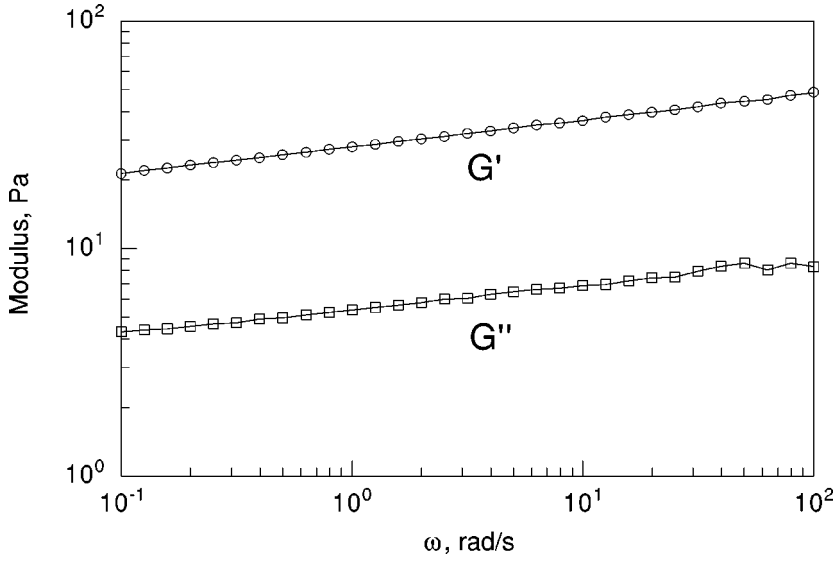

FIG. 9. Shear: dynamic rate sweep. The frequency dependence of the storage and loss moduli of type I collagen gel was tested in oscillatory shear at a constant strain amplitude of 1.0%. The data show a moderate increase in both moduli with increasing frequency.

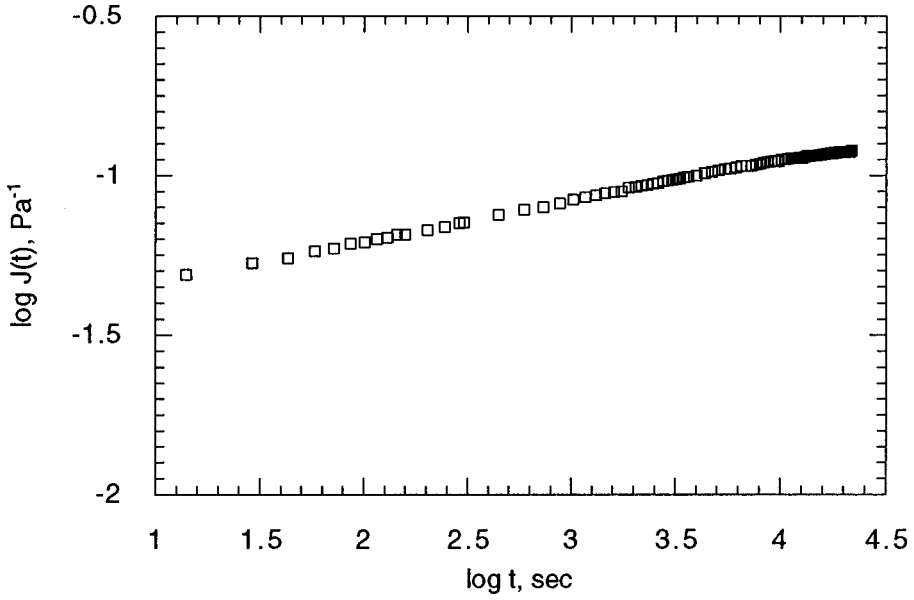

FIG. 10. Shear: creep test results. A creep test was performed at 0.70 Pa similar to those described in Barocas *et al.* (1995). The slope, m, of $\log J(t)$ vs $\log t$ was determined for the interrelation of creep compliance and dynamic modulus of collagen gel, and $m = 0.125$.

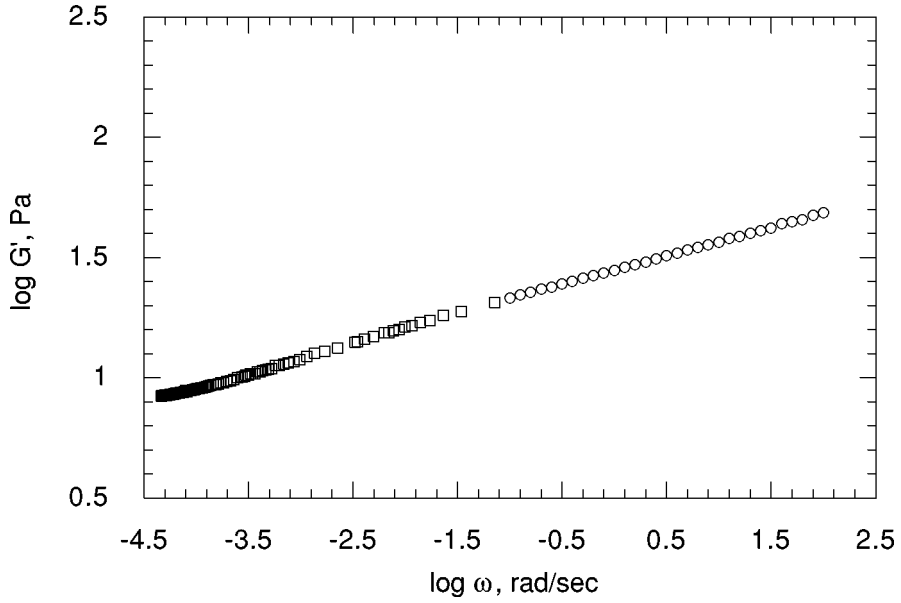

FIG. 11. Shear: comparison of creep compliance to dynamic tests. The converted creep compliance data of Fig. 10 (squares) and the dynamic data of Fig. 9 (circles) are plotted together, allowing examination of the viscoelastic behavior of collagen gel over seven logarithmic frequency decades.

D. Shear: Dynamic test, creep test, and the relaxation spectrum

The frequency dependence of G' and G'' at 1.0% shear strain is shown in Fig. 9 for angular frequencies, ω, ranging from 0.1 to 100 rad/s. Both moduli increase with ω over three logarithmic decades, reflecting finite viscoelastic relaxation mechanisms with reciprocal time constants in this region (10^{-2}–10 s). As both moduli increase in parallel, the loss tangent, G''/G', is nearly constant (0.19) over the frequency range investigated.

A creep test conducted at 0.7 Pa and maximum strain of 10%, within the linear viscoelastic regime for shear as previously reported in Barocas *et al.* (1995), is shown in Fig. 10. The plot of log $J(t)$ versus log t is linear with slope $m = 0.125$. The approximation formula given in Eq. (9) was, thus, used to convert the $J(t)$ data shown in Fig. 10 to $G'(\omega)$. These converted creep data are compared to the dynamic data of Fig. 9 in Fig. 11. The agreement of the data is quite good, and the creep and dynamic tests together describe the shear behavior of the collagen gel over nearly seven logarithmic frequency decades. The relaxation spectrum calculated from Eqs. (10) and (11) using the data in Fig. 11 is plotted in Fig. 12. The term $H(\lambda)\psi(m_1)|_{\lambda = t}$ was found to be only 10% of $G(t)$ at most, justifying the use of Eq. (9).

V. DISCUSSION

All of the confined compression tests were conducted using a Chatillon Vitrodyne V200 materials testing instrument. As this is the first reported quantitative testing of this kind done using the V200 to our knowledge, a brief discussion of the experimental difficulties encountered using this instrument is in order. The fine resolution of the force sensors on the Vitrodyne was $\pm$ 0.01 gf (0.1% of the maximum capacity of the transducer). The creep tests were performed near the low end of the range of the transducer in order to stay within the linear viscoelastic range determined for the material in shear,

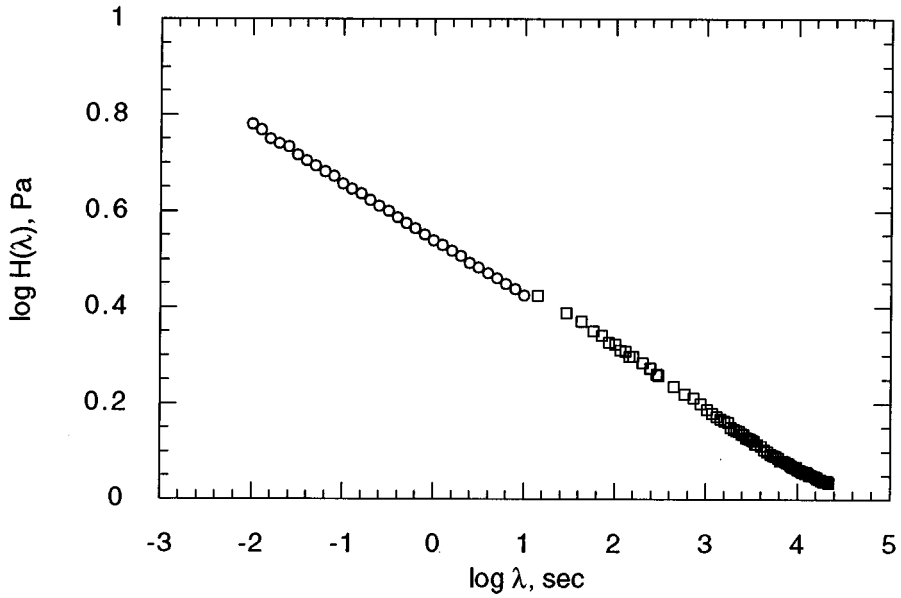

FIG. 12. Spectral relaxation function for collagen gel. The spectral relaxation function, $H(\lambda)$, of collagen gel was calculated from oscillatory shear (circles) and shear creep (squares) data from Eqs. (10) and (11), respectively, demonstrating a broad distribution of relaxation times.

reducing the ability of the controller to maintain the load at the specified settings. In addition, drift in the zero load condition during the experiment had a significant effect on the results at longer times for the creep tests. Therefore, testing at lower loads was complicated, as the combined accuracy of the load sensors and the continuing drift of zero in the load resulted in significant error in the prescribed load. As a result, the experimental error in the controlled load during the creep tests was approximately 10%, with very little contribution from the variation in the length readings (the length transducer measures within an accuracy of 3 μm, or $\sim$ 1% of the total change in length over the course of the experiment). In addition, the drift of the zero load reading made testing creep recovery impossible, as there was no way to measure the true zero load state of the material.

The short-time ramp and dynamic tests generated significantly more force than was applied in the long-time creep tests due to higher relative velocities between the solution and network phases. As a result, the experimental error in the force readings on the V200 was on the same order as the errors in the length transducer, or about $\pm$ 1% of the total reading. The repeatability of these tests was, therefore, far better than those seen in the creep test. However, the applicability of results from the short-time tests to models of compacting tissue equivalents is limited due to the incongruent time scales, whereas the creep test results (which occur over hours) are relevant.

The creep of collagen gel in compression differed both qualitatively and quantitatively from the creep seen in shear. The short-time creep of the gel in shear and compression is compared in Fig. 4. The steep initial rise in the compliance in shear as compared to the creep test can be explained by considering the flow of the interstitial solution over the network fibrils. In the compression test, the permeability of the gel (inverse of φ_0) was very important at the start of the test, resulting in the dissipation of much of the stress through the interstitial flow of solution through the collagen network as well as the

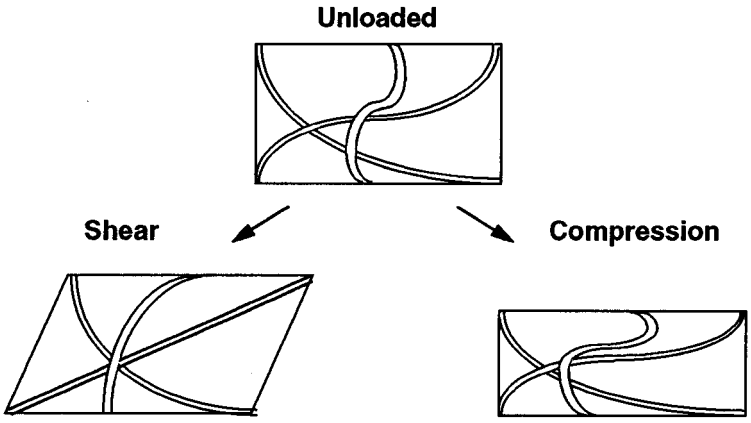

FIG. 13. Microstructural model for collagen gel deformations. This schematic of a collagen gel in shear and compression shows how fibrils are extended in shear while they buckle in confined compression. These differences in microstructural deformation can affect the macroscopic mechanical properties of the gel.

modulus [Fig. 5(b)]. As the test progressed, the deformation of the network became more important, and the viscosity of the collagen network dominated the mechanics of the gel. In shear, the network and solution phases moved together, minimizing the effects of the interstitial flow and resulting in a steep initial rise in the compliance of the gel due to the elastic contribution from the viscoelastic network.

For Poisson's ratio between 0.0 and 0.25, which is typical for inorganic gels [Scherer *et al.* (1988)], Eq. (4) predicts that the aggregate modulus measured in confined compression should be two to three times greater than the shear modulus. The actual aggregate modulus for the creep test, however, was less than half of the previously determined shear modulus, 15.5 Pa [Barocas *et al.* (1995)]. These differences were independent of the effects of the interstitial flow, as our model accounts for this effect. Therefore, we considered the differences in the microstructure of the gel in order to explain the relative weakness of the network in compression. A cartoon of an idealized section of the gel under shear and confined compression, shown in Fig. 13, shows the proposed reaction of the collagen fibril to the deformation [cf. Fig. 21 of Mow *et al.* (1992)]. In shear, the deformation is extensional in part, resulting in a tensile component in the force imposed on the fibril. Collagen fibers are known to be very strong in tension, with a tensile modulus of 100–1000 MPa [Farquhar *et al.* (1990); Fung 1993; Schwartz *et al.* (1994)]. Therefore, small strain deformation of the gel in shear must be due, in a large part, to a rearrangement or sliding of the collagen fibrils relative to one another. However, in compression, the fibrils buckle under the deformation, with no extensional component. The force required to buckle the collagen fibril is much less than is needed to stretch it [e.g., p. 333 of Lanir (1980)], resulting in a higher modulus and viscosity in shear than compression.

Although obtaining accurate creep results in compression is difficult using standard methods for collagen gels, these long-time small strain tests are most applicable to applications involving cell traction induced compaction of tissue equivalents. Usually, this process occurs over a time scale of hours, with the cells exerting a steady load, resulting in exudation of the solution from the gel. Comparing parameter estimates from the short-time ramp and long-time creep tests, however, we observe the material properties of the collagen gel change drastically with the time scale of the deformation. Whereas

results from both tests validate our assumption of Maxwell fluid behavior in compression by virtue of the goodness of fit, the modulus determined in the 120 s ramp test is 50 times higher than that estimated in the 5 hr creep test. This implies a spectrum of relaxation times (the viscosity was essentially constant for the two cases) in which the high modulus, short relaxation time processes are not observable in long-time tests, whereas they define the response of the material in the short-time tests. This is consistent with the broad relaxation spectrum determined from the shear tests (Fig. 12).

It is noteworthy that ''coarse fibrin clots,'' which share a similar network microstructure to the collagen gels studied, exhibit a similar relaxation spectrum in shear, whereas ''fine fibrin clots,'' which have smaller fiber diameters as well as a different microstructure (fibers emanating from starlike aggregates) exhibit a different relaxation spectrum (biphasic) [Gerth *et al.* (1974)]. Just as fibrin clots with different properties can be made from the same fibrinogen monomer by using different fibrillogenesis conditions, the same is true for the type I collagen monomer. We intentionally prepared the gels used in this study identically (as possible) to the way we have prepared the gels in our published studies for our applications (see citations in the introduction), since we are concerned with the compressive properties of the gel when in a form that we use for our applications (which, being stored and prepared in the manner suggested by the supplier, is presumably of similar form to that used by many other investigators using Vitrogen 100). Our ability to demonstrate acceptable reproducibility, as shown in Tables I and II, lends credence to the assertion that the reported parameter estimates are representative of collagen gels prepared from Vitrogen 100. Further, our compression data for gels prepared from different supplier lots after different periods of storage (which is always limited in our laboratory so that property changes due to storage are minimized), albeit limited, indicated no more variability than from repeated tests using gels prepared from the same lot on the same day (data not shown). Thus, although Vitrogen 100 variability is a valid concern, we have not observed significant consequences on the gel rheology.

The response of the collagen gel to dynamic tests of strains varying up to 30% was evaluated (Fig. 8). Note that minimal irreversible damage was done to the gel or gel–platen adhesion as the tests, at 2% strain at the start and end of the run, were essentially identical. The good agreement between the model predictions and experiment up to 15% implies that compressive strains below this value result lie within the LVE regime for collagen gel. This is of importance in modeling quantitative tests of cell behavior in collagen gels, as the cell-induced compaction of the gel should not be modeled out to times at which the gel has been deformed past the LVE limit unless a more complicated (nonlinear) constitutive equation is used. Tests conducted at maximum strains higher than 30% began to result in irreversible damage to the gel–platen interface, suggested by a gradual attenuation of the positive force readings over time on the V200.

Since the total time period to conduct the strain sweep [Fig. 8(a)] was 6 h, due to an equilibration period allotted before the test at each strain, any further changes in the network microstructure after 3 h were not of significant consequence for the gel compression rheology [unpublished shear data revealed G' was also nearly constant after 3 h (Moon 1992)]. Moreover, we are interested in the gel properties at the time when cells mechanically interact with the gel, which becomes significant on the time scale of 3–9 h [Barocas *et al.* (1995); Barocas and Tranquillo (1997a)]. So for both reasons, the 3h equilibration is justified.

The work of Mow and co-workers to characterize the response of articular cartilage to compressive loads using confined compression forms a good basis for comparison of our creep results. Our application of the biphasic theory is similar to that used in the Kuei–Lai–Mow (KLM) biphasic theory [Kwan *et al.* (1990)], excepting the use of the Maxwell

fluid constitutive equation rather than the elastic solid to model the mechanics of the collagen network. The differences between cell-populated collagen gel and articular cartilage [e.g., high collagen concentration, presence of proteoglycan gel in cartilage; see Barocas and Tranquillo (1994)] motivate these assumptions.

To our knowledge, this is the first estimate of the permeability of collagen gel. Our estimated value for the gel permeability ($\sim 2 \times 10^{-9}$ cm^2 estimated from the creep tests) is consistent with permeability measurements made on fibrin clots of similar network concentration by van Gelder *et al.* (1993). For creeping flows, the permeability scales with δ_p^2/η_s where δ_p is the interfibril spacing and η_s is the viscosity of the interstitial solution [Happel and Brenner (1986)], which is 0.001 Pa s for the aqueous solution in the collagen gel. Based on this analysis, we estimate an interfibrillar spacing of approximately 1 μm, which is in agreement with values obtained through diffusion measurements by Saltzman *et al.* (1994) and morphometry of SEM images [Heath and Hedlund (1984)]. Using the rheological tests we have described and given the performance limitations of the V200 (i.e., a upper frequency limit of 1 Hz in the dynamic test), it is impossible to distinguish between the viscous drag of the solution through the collagen network and other retardation processes intrinsic to the network. For example, a modified model using a constitutive equation for the network with two relaxation times [in Eq. (3)] instead of one with interphase friction [in Eq. (2)] yielded very similar fits of the creep data (not shown). However, the agreement between independent measures of the permeability and porosity, as well as the qualitative differences measured in shear versus compression (Fig. 4) validates our model assumption that both interphase drag and network viscosity are significant. Further, the parametric sensitivity analysis of the creep test fit [Fig. 5(b)] indicates that the estimates of φ_0 and η are not very interdependent because their sensitivities are most significant at different times during the test.

The goodness of fit afforded by our biphasic model is consistent with a Maxwell fluid constitutive equation for the collagen network in shear and compression. If there is a yield stress for the network, it must be below the limit of our ability to apply stress. Similarly, if there is some deviation from our assumed initial conditions (clearly, there is fibril alignment in a small layer next to all surfaces), it must not be so significant as to affect our ability to fit the data. Further, while a micromechanical/structural model would be of future interest, the conclusion is that our present model adequately represents the gel rheology for the conditions we examined. While we have used a single relaxation time version of the constitutive equation, which is motivated by and valid for the long time scale of our applications involving cell traction induced network deformation, the relaxation spectra obtained in shear (Fig. 12) and indicated for compression (i.e., the dependence of modulus on the time scale of the test) obviously imply a continuous relaxation time Maxwell fluid constitutive equation for the general case [Ferry (1980)].

The confined compression test has provided a simple and easily evaluated framework to test the validity of our biphasic theory as it applies to tissue-equivalent mechanics. The one-dimensional form of the field equations can be applied successfully to other relevant problems (our studies of cell traction forces generated in uniformly cell-populated collagen gel spheres, for example; see Barocas *et al.* (1995)). However, many relevant problems in tissue and cellular engineering are inherently two- or three-dimensional in nature, complicating the finite element analysis of the problem significantly, as well as increasing the size of the problem. We have applied the theory to a two-dimensional extension of the present problem, namely, of unconfined compression of cylindrical collagen gel samples, which enables determination of Poisson's ratio, ν. Other axisymmetric problems of interest include modeling of the compaction of dermal equivalents [Lopez Valle *et al.* (1992)] and arterial media equivalents [Weinberg and Bell (1986)]. We have

applied our theory to these problems, incorporating the effect of fibril alignment due to anisotropic network strain on cell contact guidance [Barocas and Tranquillo (1997a); Barocas and Tranquillo (1997b).

VI. CONCLUSIONS

Reconstituted type I collagen gel exhibits Maxwell fluid behavior in both shear and compression consistent with a spectrum of relaxation times, although the modulus in shear at any time scale (frequency) is larger. This difference is consistent with a random network microstructure in which some fibrils under shear are placed in tension yielding a larger modulus, whereas fibrils bend under compression yielding a smaller modulus.

ACKNOWLEDGMENTS

This work has been supported by NIH Grant No. R29-GM4052 (R.T.T.), NSF Grant No. CCR-9527151 (L.R.P.), NSF Research Training Grant No. BIR-9413241 (Traineeship to D.M.K.), and Minnesota Supercomputer Institute grants (R.T.T. and L.R.P.). The authors are grateful for the assistance of Dr. Stefano Guido and Tim Girton in obtaining the light microscopic and SEM images. The technical assistance of Tim Johnson, David Bleckinger, and Danwood Rasmussen is also gratefully acknowledged.

APPENDIX: FEM FORMULATION

The discretization of Eqs. (1)–(3) was accomplished using the standard Galerkin FEM and piecewise quadratic basis functions. The equations are in a Lagrangian reference frame, so the nodes of the discretization must move as the network deforms (recall that all material derivatives in Eqs. (1)–(3) are for points moving with network velocity, v). Thus, we defined the position of node i at time t by $u_i(t)$:

$$u_i(t) = u_{i,t=0} + \int_0^t v_i(t')dt' \Rightarrow v_i = \dot{u}_i \tag{A1}$$

(note this relation between velocity and displacement is strictly true for the Lagrangian reference frame only, while it is true only in the small-strain limit in the Eulerian frame). The discretized equations Eqs. (1)–(3) then formed an ODE system of three variables, position (u_z), stress (σ_{zz}), and network volume fraction (θ), and their time derivatives at each node. Since the creeping flow limit implicit in Eq. (2) has no acceleration dependence, we treated the velocity as a time derivative rather than a separate variable without introducing any second derivatives.

Because the computational mesh deformed, we employed an isoparametric mapping between the spatial variable z and a transformed variable $\xi \in [0,1]$. The mapping is implemented readily, since the nodal positions are variables and can be expressed as functions of the local basis functions Φ_i,

$$u = \sum_{i=1}^{n} u_i \Phi_i(\xi), \tag{A2}$$

where n is the number of nodes per element. The necessary integrals were evaluated locally using three-point Gauss quadrature in ξ space, leading to the final discretized equations. The DASOPT subroutines were then used to integrate the resulting ODE system.

References

Allen, T. D., S. L. Schor, and A. M. Schor, ''An ultrastructural review of collagen gels, a model system for cell–matrix, cell–basement membrane and cell–cell interactions,'' Scanning Electron Microsc. **1**, 375–390 (1984).

Bale, M. D., M. F. Muller, and J. D. Ferry, ''Rheological studies of creep and creep recovery of unligated fibrin clots: comparison of clots prepared with thrombin and ancrod,'' Biopolymers **24**, 461–482 (1985).

Barocas, V. H., A. G. Moon, and R. T. Tranquillo, ''The fibroblast-populated collagen microsphere assay of cell traction force-Part 2. Measurement of the cell traction parameter,'' J. Biomech. Eng. **11**, 161–170 (1995).

Barocas, V. H. and R. T. Tranquillo, ''Biphasic theory and *in vitro* assays of cell–fibril mechanical interactions in tissue-equivalent collagen gels,'' in *Cell Mechanics and Cellular Engineering*, edited by V. C. Mow, F. Guilak, R. Tran-Son-Tay, and R. M. Hochmuth (Springer-Verlag, New York, 1994), pp. 185–209.

Barocas, V. H. and R. T. Tranquillo, ''A finite element solution for the anisotropic biphasic theory of tissue-equivalent mechanics: the effect of contact guidance on isometric cell traction measurement,'' J. Biomech. Eng. **119**, 261–269 (1997a).

Barocas, V. H. and R. T. Tranquillo, ''An anisotropic biphasic theory of tissue-equivalent mechanics: The interplay among cell traction, fibril network deformation, and contact guidance,'' J. Biomech. Eng. **119**, 137–145 (1997b).

Bell, E., H. P. Ehrlich, S. Sher, C. Merrill, R. Sarber, B. Hull, T. Nakatsuji, D. Church, and D. J. Buttle, ''Development and use of a living skin equivalent,'' Plast. Reconstr. Surg. **67**, 386–392 (1981).

Bell, E., B. Ivarsson, and C. Merrill, ''Production of a tissue-like structure by contraction of collagen lattices by human fibroblasts of different proliferative potential *in vitro*,'' Proc. Natl. Acad. Sci. **76**, 1274–1278 (1979).

Dembo, M. and F. Harlow, ''Cell motion, contractile networks, and the physics of interpenetrating reactive flow,'' Biophys. J. **50**, 109–121 (1986).

Draper, N. R. and H. Smith, *Applied Regression Analysis* (Wiley, New York, 1981), pp. 458–517.

Drew, D. A. and L. A. Segel, ''Averaged equations for two-phase flows,'' Stud. Appl. Math. **1**, 205–231 (1971).

Farquhar, T., P. R. Dawson, and P. A. Torzilli, ''A microstructural model for the anisotropic drained stiffness of articular cartilage,'' J. Biomech. Eng. **112**, 414–425 (1990).

Ferry, J. D., *Viscoelastic Properties of Polymers* (Wiley, New York, 1980).

Fung, Y. C., *Biomechanics: Mechanical Properties of Living Tissue* (Springer-Verlag, New York, 1993).

Gerth, C., W. W. Roberts, and J. D. Ferry, ''Rheology of Fibrin Clots. II. Linear Viscoelastic Behavior in Shear Creep,'' Biophys. Chem. **2**, 208–217 (1974).

Grinnell, F., ''Fibroblast Reorganization of Three-Dimensional Collagen Gels and Regulation of Cell Biosynthetic Function,'' in *Fundamental Investigations on the Creation of Biofunctional Materials*, edited by S. Okamura, S. Tsuruta, Y. Imanishi, and J. Sunamoto (Kagaku-Dojin, Kyoto, 1991), pp. 33–43.

Guido, S. and R. T. Tranquillo, ''A Methodology for the Systematic and Quantitative Study of Cell Contact Guidance in Oriented Collagen Gels,'' J. Cell Sci. **105**, 317–331 (1993).

Happel, J. and H. Brenner, *Low Reynolds Number Hydrodynamics* (Martinus Nijhoff, Boston, 1986).

Heath, J. P. and K. O. Hedlund, ''Locomotion and cell surface movements of fibroblasts in fibrillar collagen gels,'' Scanning Electron Microsc. **4**, 2031–2043 (1984).

Holmes, M. H., ''Finite deformation of soft tissue: Analysis of a mixture model in uni-axial compression,'' J. Biomech. Eng. **108**, 372–381 (1986).

Kwan, M. K., W. M. Lai, and V. C. Mow, ''A finite deformation theory for cartilage and other soft hydrated connective tissues-I. Equilibrium results,'' J. Biomech. **23**, 145–155 (1990).

Lanir, Y., ''A microstructure model for the rheology of mammalian tendon,'' J. Biomech. Eng. **102**, 332–339 (1980).

Lopez Valle, C. A., F. A. Auger, R. Rompre, V. Bouvard, and L. Germain, ''Peripheral anchorage of dermal equivalents,'' British J. Derm. **127**, 365–371 (1992).

Maly, T. and L. R. Petzold, ''Numerical methods and software for sensitivity analysis of differential-algebraic systems,'' Appl. Numer. Math. **20**, 57–79 (1996).

Moon, A. G., ''Cell traction forces exerted on the extracellular matrix: Modeling and measurement,'' Ph.D. thesis, University of Minnesota (1992).

Moon, A. G. and R. T. Tranquillo, ''The fibroblast-populated collagen microsphere assay of cell traction force-Part 1. Continuum model,'' AIChE J. **39**, 163–177 (1993).

Mow, V. C., A. Ratcliffe, and A. R. Poole, ''Cartilage and diarthrodial joints as paradigms for hierarchical materials and structures,'' Biomaterials **13**, 67–97 (1992).

Petzold, L. R., ''A description of DASSL: a differential/algebraic system solver,'' in *Scientific Computing: Applications of Mathematics and Computing to the Physical Sciences*, edited by R. S. Stepleman (North-Holland, Amsterdam, 1983), pp. 65–68.

Petzold, L. R., J. B. Rosen, P. E. Gill, L. O. Jay, and K. Park, ''Numerical Optimal Control of Parabolic PDEs using DASOPT,'' in *Large Scale Optimization with Applications, Part II: Optimal Design and Control*,

IMA Volumes in Mathematics and its Applications, Vol. 93, edited by L. T. Biegler, T. F. Coleman, A. R. Conn, and F. N. Santosa (Springer-Verlag, New York, 1997), pp. 271–300.

Saltzman, W. M., M. L. Radomsky, K. J. Whaley, and R. A. Cone, ''Antibody diffusion in human cervical mucus,'' Biophys. J. **66**, 508–515 (1994).

Scherer, G. W., S. A. Pardenek, and R. M. Swiatek, ''Viscoelasticity in silica gel,'' J. Non-Cryst. Solids **108**, 14–22 (1988).

Schwartz, M., P. H. Leo, and J. L. Lewis, ''A microstructural model of articular cartilage,'' J. Biomech. **27**, 865–873 (1994).

Setton, L. A., W. Zhu, and V. C. Mow, ''The biphasic poroviscoelastic behavior of articular cartilage: Role of the surface zone in governing the compressive behavior,'' J. Biomech. **26**, 581–592 (1993).

Tranquillo, R.T., T. S. Girton, B. A. Bromberek, T. G. Triebes, and D. L. Mooradian, ''Magnetically orientated tissue-equivalent tubes: Application to a circumferentially orientated media-equivalent,'' Biomaterials **17**, 349–357 (1996).

Tschoegl, N. W., *The Phenomenological Theory of Linear Viscoelastic Behavior* (Springer-Verlag, Berlin, 1989).

van Gelder, J. M., C. H. Nair, and D. P. Dhall, ''Effects of poloxamer 188 on fibrin network structure, whole blood clot permeability and fibrinolysis,'' Thrombosis Research **71**, 361–76 (1993).

Weinberg, C. B. and E. Bell, ''A blood vessel constructed from collagen and cultured vascular cells,'' Science **231**, 397–400 (1986).